

Fabrication of sulfur-doped cove-edged graphene nanoribbons on Au(111)

Huan Yang(杨欢), Yixuan Gao(高艺璇), Wenhui Niu(牛雯慧), Xiao Chang(常霄), Li Huang(黄立), Junzhi Liu(刘俊治), Yiyong Mai(麦亦勇), Xinliang Feng(冯新亮), Shixuan Du(杜世萱), and Hong-Jun Gao(高鸿钧)

Citation: Chin. Phys. B, 2021, 30 (**7**): 077306. DOI: 10.1088/1674-1056/abfbd0

Journal homepage: http://cpb.iphy.ac.cn; http://iopscience.iop.org/cpb

What follows is a list of articles you may be interested in

Twistronics in graphene-based van der Waals structures

Ya-Ning Ren(任雅宁), Yu Zhang(张钰), Yi-Wen Liu(刘亦文), and Lin He(何林)

Chin. Phys. B, 2020, 29 (**11**): 117303. DOI: 10.1088/1674-1056/abbbe2

Probing the Majorana bound states in a hybrid nanowire double-quantum-dot system by scanning tunneling microscopy

Jia Liu(刘佳), Ke-Man Li(李科曼), Feng Chi(迟锋), Zhen-Guo Fu(付振国), Yue-Fei Hou(侯跃飞), Zhigang Wang(王志刚), Ping Zhang(张平)

Chin. Phys. B, 2020, 29 (**7**): 077302. DOI: 10.1088/1674-1056/ab8889

Epitaxial fabrication of monolayer copper arsenide on Cu(111)

Shuai Zhang(张帅), Yang Song(宋洋), Jin Mei Li(李金梅), Zhenyu Wang(王振宇), Chen Liu(刘晨), Jia-Ou Wang(王嘉鸥), Lei Gao(高蕾), Jian-Chen Lu(卢建臣), Yu Yang Zhang(张余洋), Xiao Lin(林晓), Jinbo Pan(潘金波), Shi Xuan Du(杜世萱), Hong-Jun Gao(高鸿钧)

Chin. Phys. B, 2020, 29 (**7**): 077301. DOI: 10.1088/1674-1056/ab8db3

Scanning tunneling microscopic investigation on morphology of magnetic Weyl semimetal $YbMnBi_2$

Zhen Zhu(朱朕), Dong Yan(严冬), Xiao-Ang Nie(聂晓昂), Hao-Ke Xu(徐豪科), Xu Yang(杨旭), Dan-Dan Guan(管丹丹), Shiyong Wang(王世勇), Yao-Yi Li(李耀义), Canhua Liu(刘灿华), Jun-Wei Liu(刘军伟), Hui-Xia Luo(罗惠霞), Hao Zheng(郑浩), Jin-Feng Jia(贾金锋)

Chin. Phys. B, 2019, 28 (**7**): 077302. DOI: 10.1088/1674-1056/28/7/077302

Image charge effect on the light emission of rutile TiO_2(110) induced by a scanning tunneling microscope

Chaoyu Guo(郭钞宇), Xiangzhi Meng(孟祥志), Qin Wang(王钦), Ying Jiang(江颖)

Chin. Phys. B, 2018, 27 (**7**): 077301. DOI: 10.1088/1674-1056/27/7/077301

Fabrication of sulfur-doped cove-edged graphene nanoribbons on Au(111)*

Huan Yang(杨欢)[1,†], Yixuan Gao(高艺璇)[1,†], Wenhui Niu(牛雯慧)[2,3,†], Xiao Chang(常霄)[1], Li Huang(黄立)[1,‡], Junzhi Liu(刘俊治)[2,4], Yiyong Mai(麦亦勇)[3], Xinliang Feng(冯新亮)[2,§], Shixuan Du(杜世萱)[1,5,¶], and Hong-Jun Gao(高鸿钧)[1,5]

[1] *Institute of Physics and University of Chinese Academy of Sciences (CAS), Beijing* 100190, *China*
[2] *Center for Advancing Electronics Dresden (cfaed) & Faculty of Chemistry and Food Chemistry, Technische Universität Dresden*, 01062 *Dresden, Germany*
[3] *School of Chemistry and Chemical Engineering, Frontiers Science Center for Transformative Molecules, Shanghai Key Laboratory of Electrical Insulation and Thermal Ageing, Shanghai Jiao Tong University, Shanghai* 200240, *China*
[4] *Department of Chemistry and State Key Laboratory of Synthetic Chemistry, The University of Hong Kong, Hong Kong, China*
[5] *CAS Center for Excellence in Topological Quantum Computation, University of Chinese Academy of Sciences, Beijing* 100190, *China*

(Received 1 April 2021; revised manuscript received 22 April 2021; accepted manuscript online 27 April 2021)

The on-surface synthesis from predesigned organic precursors can yield graphene nanoribbons (GNRs) with atomically precise widths, edge terminations and dopants, which facilitate the tunning of their electronic structures. Here, we report the synthesis of novel sulfur-doped cove-edged GNRs (S-CGNRs) on Au(111) from a specifically designed precursor containing thiophene rings. Scanning tunneling microscopy and non-contact atomic force microscopy measurements elucidate the formation of S-CGNRs through subsequent polymerization and cyclodehydrogenation, which further result in crosslinked branched structures. Scanning tunneling spectroscopy results reveal the conduction band minimum of the S-CGNR locates at 1.2 eV. First-principles calculations show that the S-CGNR possesses an energy bandgap of 1.17 eV, which is evidently smaller than that of an undoped cove-edged GNR (1.7 eV), suggesting effective tuning of the bandgap by introducing sulfur atoms. Further increasing the coverage of precursors close to a monolayer results in the formation of linear-shaped S-CGNRs. The fabrication of S-CGNRs provides one more candidate in the GNR toolbox and promotes the future applications of heteroatom-doped graphene nanostructures.

Keywords: on-surface synthesis, sulfur-doped cove-edged graphene nanoribbons, scanning tunneling microscopy, non-contact atomic force microscopy

PACS: 73.22.Pr, 68.37.Ef, 85.65.+h, 71.15.Mb **DOI:** 10.1088/1674-1056/abfbd0

1. Introduction

Graphene has attracted intensive attentions due to its unique properties and potential applications in nanoelectronics.[1–7] Graphene nanoribbons (GNRs), which have an energy bandgap and tunable electronic structures,[4,8–11] that can be directly determined by widths, edge configurations, and dopants are an important branch in graphene research as promising candidates for future electronic devices.[12–18] The fabrication of GNRs generally includes top-down and bottom-up approaches,[19–22] among which the latter is renowned for its capabilities to yield structurally well-defined GNRs.[19,23,24] With specifically designed organic precursors, scientists have achieved various kinds of GNRs, including armchair-edged GNRs with different widths and their corresponding heterostructures,[15,19,25,26] zigzag-edged GNRs, and cove-edged GNRs.[16,27–29] Among those, cove-edged GNRs as a representative semiconductor enrich the families of GNRs, which could benefit to explore exotic physical properties of GNRs containing distinct edge configurations.[27,30,31] Furthermore, GNRs doped with heteroatoms have been successfully synthesized and investigated during the past few years.[12,32–34] For instance, the introduction of nitrogen (N) atoms into the GNRs can shift the bandgap position without changing its magnitude;[12,33,35] while sulfur (S) and boron (B) atoms can lead to the change of the bandgap values of GNRs.[36–40] Particularly, bandgaps of GNRs can be further tailored by modulating sulfur configurations, which may yield S-doped GNRs containing a sequence of multiple heterojunc-

*Project supported by the National Natural Science Foundation of China (Grant Nos. 51761135130, 61888102, and 21774076), the National Key Research and Development Program of China (Grant Nos. 2018YFA0305800 and 2019YFA0308500), the DFG EnhanceNano (Grant No. 391979941), the Strategic Priority Research Program of Chinese Academy of Sciences (Grant Nos. XDB30000000), the International Partnership Program of Chinese Academy of Sciences (Grant No. 112111KYSB20160061), and the K C Wong Education Foundation and the Program of Shanghai Academic Research Leader (Grant No. 19XD1421700).

†These authors contributed equally to this work.
‡Corresponding author. E-mail: lhuang@iphy.ac.cn
§Corresponding author. E-mail: xinliang.feng@tu-dresden.de
¶Corresponding author. E-mail: sxdu@iphy.ac.cn

© 2021 Chinese Physical Society and IOP Publishing Ltd

tions with distinct bandgaps.[37,38]

In this work, we report the bottom-up synthesis of sulfur-doped cove-edged graphene nanoribbons (S-CGNRs) on Au(111) using a uniquely designed thiophene-ring containing precursor, 4,4'-dibromo-10,10'-biphenanthro[2,1-*b*]thiophene (DBDPT). Scanning tunneling microscopy (STM) measurements verified the successful fabrication of GNRs, while non-contact atomic force microscopy (nc-AFM) images confirmed the existence of S dopants at the cove edges. Scanning tunneling spectroscopy (STS) spectra demonstrate the conduction band minimum of the S-CGNR locates at 1.2 eV. Density functional theory (DFT) calculations on the well-ordered S-CGNRs show a bandgap of 1.17 eV, significantly narrower than that of the pristine carbon-based cove-edged CNRs (CGNRs) (1.7 eV).[27] Due to the partial cleavage of C–S bonds and different chirality of the precursor on the surface, the involved Ullmann-type polymerization and cyclodehydrogenation yielded S-CGNRs with branched configurations. By increasing the precursor coverage from sub-monolayer to monolayer, the cross-link of S-CGNRs was evidently reduced, providing linear-shaped S-CGNRs arrays.

2. Methods

2.1. Sample preparation, STM/STS measurement

All experiments were performed in a CreaTec ultra-high vacuum (UHV) STM/nc-AFM system with a base pressure of 2×10^{-10} mbar (1 bar = 10^5 Pa). Au(111) substrate was cleaned by repeated cycles of Ar^+ ion sputtering and annealing at 700 K for 20 min. The precursor was thermally sublimated at 560 K onto the Au(111) substrate, which was held at room temperature during molecular deposition. Subsequently, the sample was annealed at 500 K and 700 K for 40 min each, which led to the surface-assisted polymerization and cyclodehydrogenation to form corresponding polymers and S-CGNRs, respectively. All STM and nc-AFM measurements were carried out at 5 K using a qPlus tuning. STM images were obtained in constant current mode and the voltages referred to the bias on samples with respect to the tip. AFM images were acquired in the frequency modulation mode with a CO-functionalized tip.[41,42] Differential conductance ($\mathrm{d}I/\mathrm{d}V$) spectra were acquired by using a lock-in technique at a frequency of 973 Hz.

2.2. DFT calculations

The structural relaxations and electronic-structure calculations were performed within density functional theory calculations by using the Vienna *ab initio* simulation package.[43,44] A generalized gradient approximation (GGA) in the form of Perdew–Burke–Ernzerhof (PBE) generalized gradient approximation was adopted for the exchange–correlation functional.[45] The wave functions were expanded using a planewave basis set with an energy cutoff of 500 eV. The thickness of vacuum layer was larger than 13 Å to avoid interactions between neighboring nanoribbons. A Γ-centered $6 \times 1 \times 1$ k-point sampling in the first Brillouin zone was used during structural optimization of the GNR. The structures were relaxed until the residual forces were smaller than 0.01 eV/Å. The band structure was calculated along high symmetry directions in the Brillouin zone.

3. Results and discussion

Figure 1(a) illustrates the synthesis of S-CGNRs on Au(111) from a specifically designed precursor containing fused thiophene rings (4,4'-dibromo-10,10'-biphenanthro[2,1-*b*]thiophene, DBDPT, synthesis method described in Section 2 and Figs. S1–S6 of supplementary material). In principle, the precursors could undergo dehalogenation, polymerization, and cyclodehydrogenation when annealed on surface, resulting in the formation of GNRs with sulfur-doped cove edges as shown in Fig. 1(a).

The DBDPT molecules are prochiral when deposited on Au(111) substrate, as illustrated in Fig. S7(a). Due to the steric hinderance between the two groups of hydrogen atoms highlighted by the green ovals in Fig. 1(a), the precursors are not planar on the substrate. At low coverage, the precursors tend to form clusters that adsorb on fcc and elbow regions of the reconstructed Au(111) surface as shown in Fig. 1(b). Most of the clusters consist of 10 bright protrusions with a height of 320 pm (Fig. S7(c)) and assemble into rhomboids. The apparent lateral size of one bright protrusion in STM images is about 1.95 nm (Fig. S7(c)), which is comparable to the lateral size of a precursor (1.1 nm) considering the dispersed electronic states of molecules. Therefore, we attribute each bright protrusion in Fig. 1(b) corresponds to a single molecular precursor. By annealing the sample to 500 K, the precursors went through Ullmann coupling and formed polymers. The polymers defused into islands on fcc regions of Au(111) surface and modified the Au(111) surface reconstruction as shown in Fig. 1(c), suggesting a strong interaction between the polymers. Figure 1(d) shows an STM image of the sample after annealing to 700 K, which results in the formation of GNRs with a height of 180 pm (Fig. S8). Most nanoribbons exhibit an appearance of branched structures that indicate complex inter-ribbon cross-coupling during the cyclodehydrogenation stage. The straight ribbon segments generally have the lengths ranging from 2 nm to 9 nm. The strong interaction between the polymers in previous step is likely the reason for the formation of the branch-shape GNRs.

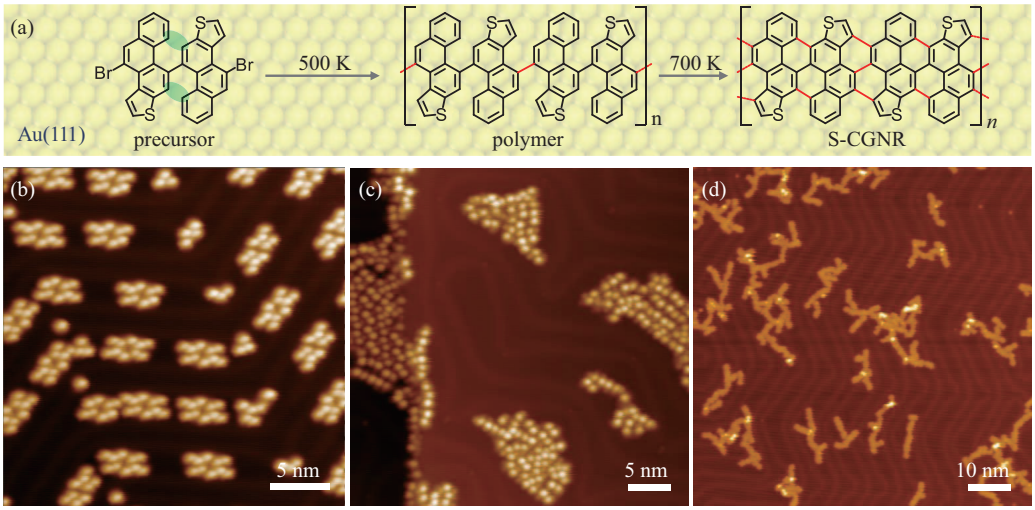


Fig. 1. On-surface synthetic process of S-CGNR and the corresponding STM images on Au(111). (a) Structure model of the precursor 4,4'-dibromo-10,10'-biphenanthro[2,1-*b*]thiophene monomer, the polymer after Ullmann reaction, and the resultant S-CGNR. (b) STM image of the precursors adsorbed on Au(111) substrate at a coverage of 0.2 ML ($V = -1$ V, $I = 10$ pA). (c) STM image of the polymers after annealing the sample to 500 K ($V = -1$ V, $I = 10$ pA). (d) STM image of the S-CGNRs after annealing the sample to 700 K ($V = -1$ V, $I = 10$ pA).

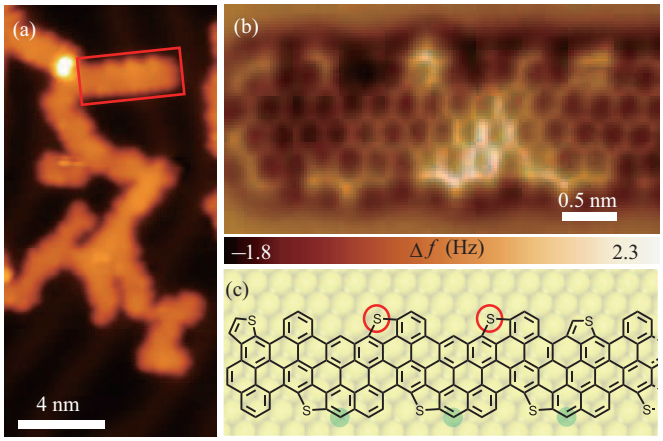


Fig. 2. A segment of branched S-CGNRs. (a) STM image of S-CGNRs ($V = -1$ V, $I = 10$ pA). (b) Chemical-bond-resolved nc-AFM image of the S-CGNR segment obtained on the area marked by a red rectangle in panel (a). (c) Structure model of the S-CGNR segment. The segment is originated from isomers with the same chirality.

Despite the branch-like morphology, it is possible to find short straight segments of GNRs that have ordered peripheries. To gain further insight into the atomic structure of the resultant ribbons, nc-AFM measurements were carried out with a CO-functionalized tip.[46] The AFM image in Fig. 2(b) is obtained on the area marked by the red rectangle in Fig. 2(a). Combining the AFM image and the configurations of the precursors, we infer that the segment in Fig. 2(b) arises from precursors with the same chirality. To guide our eyes, the corresponding structure model of the nanoribbon is provided in Fig. 2(c). The cove-shaped edges are clearly visualized, but not as uniform as illustrated in Fig. 1(a). The thiophene rings observed in the AFM image prove the existence of sulfur atoms. However, some C–S bonds have been cleaved due to annealing at high temperature and the unsaturated S atoms form new bonds with adjacent carbon atoms marked with red circles in the structure model in Fig. 2(c). Carbon atoms detached from other precursors may also be involved in the reaction to form the ribbons, as referred by the green circles (Fig. 2(c)).

For the purpose of unveiling the electronic properties of S-CGNRs, differential conductance ($\mathrm{d}I/\mathrm{d}V$) spectra were performed to obtain the local density of states (LDOS) of the ribbon. Figure 3(a) shows an STM image of a short segment from a S-CGNR, which was used to acquire the representative $\mathrm{d}I/\mathrm{d}V$ spectra. In Fig. 3(b), the red curve was taken on the S-CGNR as marked by the red dot in Fig. 3(a), while the black curve taken on bare Au(111) surface for comparison with the same tip. The significantly increased intensity of LDOS at 1.2 V is attributed to the conduction band minimum (CBM) of the S-CGNR. The valence band maximum of the S-CGNR is not detected due to the strong coupling between S-CGNRs and metallic substrate, which is similar to the situation for zigzag-edges graphene nanoribbons on Au(111).[16] Meanwhile, the spatial distribution of the CBM on the ribbon is displayed in the $\mathrm{d}I/\mathrm{d}V$ map in Fig. 3(c), exhibiting pronounced LDOS along the coved edges of the ribbon.

To explore the effect of S atoms on the electronic structures of CGNRs, DFT calculations were also carried out based on the perfect structure of S-CGNR in Fig. 1(a). Figures 3(d) shows the DFT calculated density of states (DOS) of S-CGNR, indicating a bandgap of 1.17 eV. Compared to its corresponding pristine CGNR that has been reported to have a calculated bandgap of 1.70 eV,[27] the doping of S atoms significantly reduces the energy bandgap.

In order to tune the morphology of S-CGNRs, we tried to adjust the coverage of DBBPT molecules to near monolayer. At this coverage, the precursors form self-assembled structures along the Au(111) surface reconstruction, as dis-

played in Fig. 4(a). Magnified STM image shows detailed well-ordered monolayer structure in Fig. 4(b), in which the DBBPT molecules regularly assemble to form the periodical nanoporous structures. After annealing the sample to 700 K, S-CGNRs can be obtained as shown in Fig. 4(c). Long-curved ribbons are formed comparing with the branch-like structures in sub-monolayer coverage. The zoom-in STM image in Fig. 4(d) shows that well-aligned linear-shaped S-CGNRs can also be formed in this condition, as highlighted in the red rectangle.

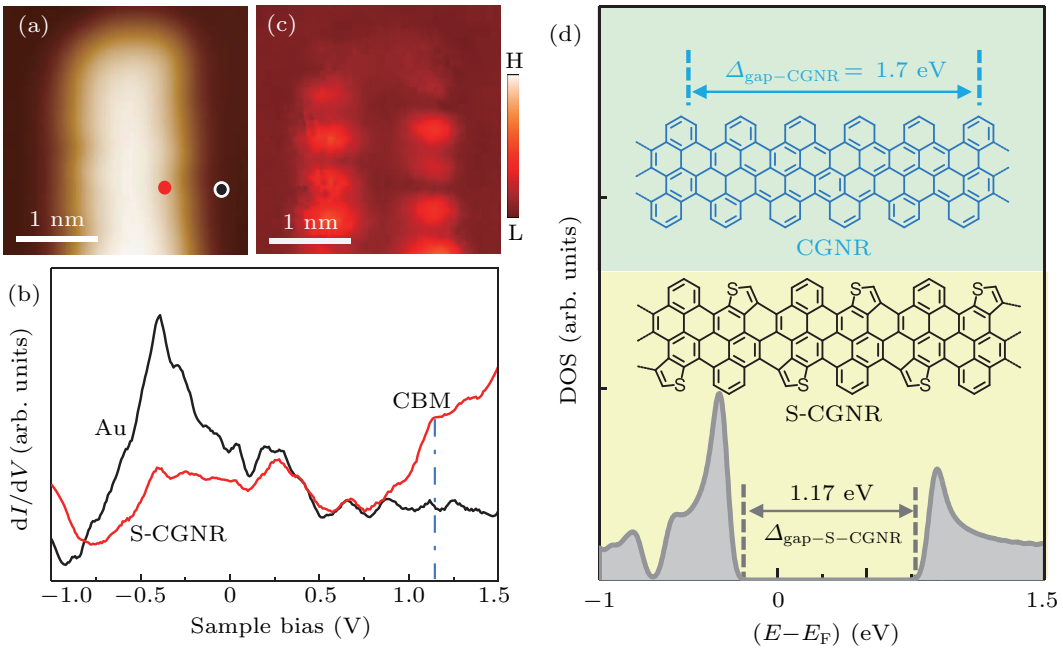


Fig. 3. Electronic structure of S-CGNR. (a) STM image of a short segment from a S-CGNR ($V = 1$ V, $I = 50$ pA). (b) Differential conductance ($\mathrm{d}I/\mathrm{d}V$) spectra taken on a S-CGNR (red) and on bare Au(111) (black). The conduction band minimum (CBM) of the S-CGNR locates at 1.2 eV (open-feedback parameters: $V = 1.00$ V, $I = 50$ pA; modulation voltage $V_{\mathrm{rms}} = 10$ mV). (c) $\mathrm{d}I/\mathrm{d}V$ map at the energy of 1.2 eV (CBM) (open-feedback parameters: $V = 1.2$ V, $I = 600$ pA, modulation voltage $V_{\mathrm{rms}} = 20$ mV). (d) DFT calculated density of states (DOS) of the S-CGNR. The DFT calculations show that the S-CGNR has a bandgap of 1.17 eV, while the pristine CGNR possesses a bandgap of 1.7 eV.

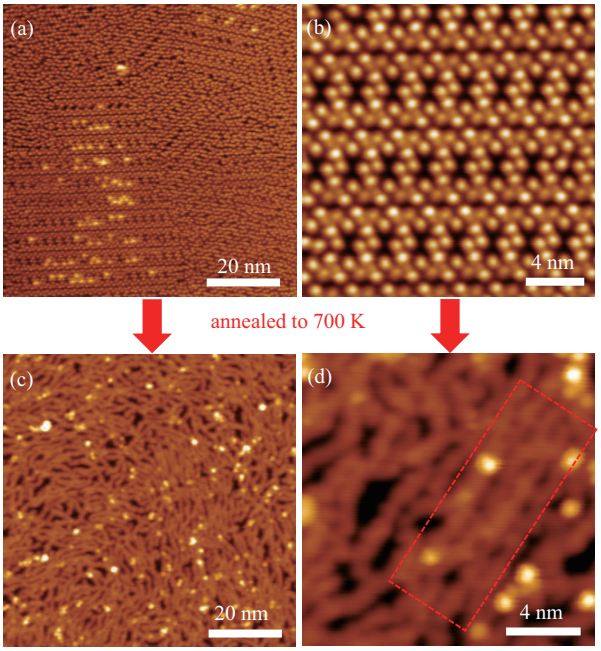


Fig. 4. STM images of monolayer precursors and the corresponding S-CGNRs on Au(111). (a) Monolayer precursors deposited on Au(111) substrate ($V = -1$ V, $I = 10$ pA). (b) Magnified STM image of monolayer precursors ($V = 1$ V, $I = 60$ pA). (c) STM image of the S-CGNRs shows linear structures after annealing to 700 K ($V = -1$ V, $I = 30$ pA). (d) Zoom-in STM image on the S-CGNRs presents the well-aligned linear-shaped structures ($V = -1$ V, $I = 30$ pA).

4. Conclusion

We have successfully synthesized sulfur-doped cove-edged GNRs on Au(111) substrate. Nc-AFM image confirms the formation of S-CGNRs and resolves the atomic structures with non-uniform edge configurations due to the C–S bond cleavage at elevated temperature. STS spectra demonstrate the conduction band minimum of the S-CGNR locates at 1.2 eV. DFT calculations reveal that the well-ordered, S-CGNRs have a bandgap of 1.17 eV, which is much smaller than that of the pristine carbon-based GNRs with the similar structure. The S-CGNRs produced with low precursor coverage cross-couple into branched structures. With increasing the precursor coverage to near monolayer, linear-shaped ribbons have been successfully obtained. This bottom-up synthesis of S-CGNRs promotes future applications of heteroatom-doped graphene nanoribbons in nanoelectronics.

Acknowledgements

Part of the research was performed in the Key Laboratory of Vacuum Physics, Chinese Academy of Sciences. Computational resources were provided by the National Supercomputing Center in Tianjin Municipality, China. The Instrumental

Analysis Center of Shanghai Jiao Tong University is also acknowledged for some measurements.

References

[1] Novoselov K S, Geim A K, Morozov S V, Jiang D, Zhang Y, Dubonos S V, Grigorieva I V and Firsov A A 2004 *Science* **306** 666

[2] Novoselov K S, Jiang D, Schedin F, Booth T J, Khotkevich V V, Morozov S V and Geim A K 2005 *Proc. Nat. Acad. Sci. USA* **102** 10451

[3] Geim A K and Novoselov K S 2007 *Nat. Mater.* **6** 183

[4] Castro Neto A H, Guinea F, Peres N M R, Novoselov K S and Geim A K 2009 *Rev. Mod. Phys.* **81** 109

[5] Ma R S, Huan Q, Wu L M, Yan J H, Zhang Y Y, Bao L H, Liu Y Q, Du S X and Gao H J 2017 *Chin. Phys. B* **26** 066801

[6] Guo H, Chen H, Que Y, Zheng Q, Zhang Y Y, Bao L H, Huang L, Wang Y L, Du S X and Gao H J 2019 *Chin. Phys. B* **28** 056107

[7] Huang L, Li G, Zhang Y Y, Bao L H, Huan Q, Lin X, Wang Y L, Guo H M, Shen C M, Du S X and Gao H J 2018 *Acta Phys. Sin.* **67** 126801 (in Chinese)

[8] Son Y W, Cohen M L and Louie S G 2006 *Phys. Rev. Lett.* **97** 216803

[9] Han M Y, Özyilmaz B, Zhang Y and Kim P 2007 *Phys. Rev. Lett.* **98** 206805

[10] Llinas J P, Fairbrother A, Borin Barin G, Shi W, Lee K, Wu S, Yong Choi B, Braganza R, Lear J, Kau N, Choi W, Chen C, Pedramrazi Z, Dumslaff T, Narita A, Feng X, Mullen K, Fischer F, Zettl A, Ruffieux P, Yablonovitch E, Crommie M, Fasel R and Bokor J 2017 *Nat. Commun.* **8** 633

[11] Su X, Xue Z, Li G and Yu P 2018 *Nano Lett.* **18** 5744

[12] Bronner C, Stremlau S, Gille M, Brausse F, Haase A, Hecht S and Tegeder P 2013 *Angew. Chem., Int. Ed.* **52** 4422

[13] Chen Y C, de Oteyza D G, Pedramrazi Z, Chen C, Fischer F R and Crommie M F 2013 *ACS Nano* **7** 6123

[14] Cai J, Pignedoli C A, Talirz L, Ruffieux P, Sode H, Liang L, Meunier V, Berger R, Li R, Feng X, Mullen K and Fasel R 2014 *Nat. Nanotechnol.* **9** 896

[15] Kimouche A, Ervasti M M, Drost R, Halonen S, Harju A, Joensuu P M, Sainio J and Liljeroth P 2015 *Nat. Commun.* **6** 10177

[16] Ruffieux P, Wang S, Yang B, Sanchez-Sanchez C, Liu J, Dienel T, Talirz L, Shinde P, Pignedoli C A, Passerone D, Dumslaff T, Feng X, Mullen K and Fasel R 2016 *Nature* **531** 489

[17] Qi C and Hu J 2018 *Chin. Phys. B* **27** 077106

[18] Xiao Y, Ye Q, Liang J, Yan X and Zhang Y 2020 *Chin. Phys. B* **29** 127201

[19] Cai J, Ruffieux P, Jaafar R, Bieri M, Braun T, Blankenburg S, Muoth M, Seitsonen A P, Saleh M, Feng X, Mullen K and Fasel R 2010 *Nature* **466** 470

[20] Wang X and Dai H 2010 *Nat. Chem.* **2** 661

[21] Magda G Z, Jin X, Hagymasi I, Vancso P, Osvath Z, Nemes-Incze P, Hwang C, Biro L P and Tapaszto L 2014 *Nature* **514** 608

[22] Kolmer M, Steiner A K, Izydorczyk I, Ko W, Engelund M, Szymonski M, Li A P and Amsharov K 2020 *Science* **369** 571

[23] Talirz L, Ruffieux P and Fasel R 2016 *Adv. Mater.* **28** 6222

[24] Nguyen G D, Tsai H Z, Omrani A A, Marangoni T, Wu M, Rizzo D J, Rodgers G F, Cloke R R, Durr R A, Sakai Y, Liou F, Aikawa A S, Chelikowsky J R, Louie S G, Fischer F R and Crommie M F 2017 *Nat. Nanotechnol.* **12** 1077

[25] Chen Y C, Cao T, Chen C, Pedramrazi Z, Haberer D, de Oteyza D G, Fischer F R, Louie S G and Crommie M F 2015 *Nat. Nanotechnol.* **10** 156

[26] Bronner C, Durr R A, Rizzo D J, Lee Y L, Marangoni T, Kalayjian A M, Rodriguez H, Zhao W, Louie S G, Fischer F R and Crommie M F 2018 *ACS Nano* **12** 2193

[27] Liu J, Li B W, Tan Y Z, Giannakopoulos A, Sanchez-Sanchez C, Beljonne D, Ruffieux P, Fasel R, Feng X and Mullen K 2015 *J. Am. Chem. Soc.* **137** 6097

[28] Wang S, Talirz L, Pignedoli C A, Feng X, Mullen K, Fasel R and Ruffieux P 2016 *Nat. Commun.* **7** 11507

[29] Wang X Y, Urgel J I, Barin G B, Eimre K, Di Giovannantonio M, Milani A, Tommasini M, Pignedoli C A, Ruffieux P, Feng X, Fasel R, Mullen K and Narita A 2018 *J. Am. Chem. Soc.* **140** 9104

[30] Gröning O, Wang S, Yao X, Pignedoli C A, Borin Barin G, Daniels C, Cupo A, Meunier V, Feng X, Narita A, Müllen K, Ruffieux P and Fasel R 2018 *Nature* **560** 209

[31] Rizzo D J, Veber G, Cao T, Bronner C, Chen T, Zhao F, Rodriguez H, Louie S G, Crommie M F and Fischer F R 2018 *Nature* **560** 204

[32] Lv R and Terrones M 2012 *Mater. Lett.* **78** 209

[33] Maaß F, Utecht M, Stremlau S, Gille M, Schwarz J, Hecht S, Klamroth T and Tegeder P 2017 *Phys. Rev. B* **96** 045434

[34] Senkovskiy B V, Usachov D Y, Fedorov A V, Marangoni T, Haberer D, Tresca C, Profeta G, Caciuc V, Tsukamoto S, Atodiresei N, Ehlen N, Chen C, Avila J, Asensio M C, Varykhalov A Y, Nefedov A, Woll C, Kim T K, Hoesch M, Fischer F R and Gruneis A 2018 *ACS Nano* **12** 7571

[35] Zhang Y, Zhang Y, Li G, Lu J, Lin X, Du S, Berger R, Feng X, Müllen K and Gao H J 2014 *Appl. Phys. Lett.* **105** 023101

[36] Kawai S, Saito S, Osumi S, Yamaguchi S, Foster A S, Spijker P and Meyer E 2015 *Nat. Commun.* **6** 8098

[37] Nguyen G D, Toma F M, Cao T, Pedramrazi Z, Chen C, Rizzo D J, Joshi T, Bronner C, Chen Y C, Favaro M, Louie S G, Fischer F R and Crommie M F 2016 *J. Phys. Chem. C* **120** 2684

[38] Zhang Y F, Zhang Y, Li G, Lu J, Que Y, Chen H, Berger R, Feng X, Müllen K, Lin X, Zhang Y Y, Du S, Pantelides S T and Gao H J 2017 *Nano Res.* **10** 3377

[39] Cao Y, Qi J, Zhang Y F, Huang L, Zheng Q, Lin X, Cheng Z, Zhang Y Y, Feng X, Du S, Pantelides S T and Gao H J 2018 *Nano Res.* **11** 6190

[40] Pedramrazi Z, Chen C, Zhao F, Cao T, Nguyen G D, Omrani A A, Tsai H Z, Cloke R R, Marangoni T, Rizzo D J, Joshi T, Bronner C, Choi W W, Fischer F R, Louie S G and Crommie M F 2018 *Nano Lett.* **18** 3550

[41] Gross L, Mohn F, Moll N, Liljeroth P and Meyer G 2009 *Science* **325** 1110

[42] Pavlicek N, Majzik Z, Collazos S, Meyer G, Perez D, Guitian E, Pena D and Gross L 2017 *ACS Nano* **11** 10768

[43] Kresse G and Furthmüller J 1996 *Phys. Rev. B* **54** 11169

[44] Kresse G and Furthmüller J 1996 *Comp. Mater. Sci.* **6** 15

[45] Perdew J P, Burke K and Ernzerhof M 1996 *Phys. Rev. Lett.* **77** 3865

[46] Bartels L, Meyer G and Rieder K H 1997 *Appl. Phys. Lett.* **71** 213